SYNTHESIS OF BOEHMITE/ORGANOMODIFIED MONTMORILLONITE COMPOSITES BY A HYDROTHERMAL METHOD: PROPERTIES AND USE FOR COATING COTTON FABRIC

MING-SHIEN YEN,[*] MU-CHENG KUO,[*] CHIEN-WEN CHEN,[*] JYH-HORNG WU[**] and JHENG-HONG WU[*]

[*]*Department of Materials Engineering, Kun Shan University, Tainan 71003, Taiwan*
[**]*Green Energy & Eco-Technology Center, Industrial Technology Research Institute, Tainan70955, Taiwan*
✉ *Corresponding author: Ming-Shien Yen, yms0410@mail.ksu.edu.tw*

Received December 29, 2014

In this study, organomodified montmorillonite (m-MMT) was prepared by the exfoliation of montmorillonite with cetyltrimethylammonium bromide, followed by secondary exfoliation after ion exchange. Boehmite/m-MMT composites were prepared by treating boehmite sol with aluminum isopropoxide using a hydrothermal method, and mixing the sol with m-MMT. The chemical compositions of the prepared composites were analyzed using Fourier transform infrared analysis, ^{29}Si nuclear magnetic resonance spectroscopy and X-ray diffraction. Cotton fabrics were coated by using a process of padding, drying and curing. The surface properties of the processed cotton fabrics were analyzed by scanning electron microscopy (SEM), and their water repellency, weatherability and conductivity were investigated. SEM analysis showed a uniform coating layer on the surface of the processed cotton fabrics. The water repellency and weatherability of the fabrics coated with boehmite/m-MMT composites improved substantially, and the conductivity increased moderately.

Keywords: boehmite, montmorillonite, cotton, water repellency, hydrothermal method, composite materials

INTRODUCTION

Inorganic–organic composite materials with well-defined nanostructures have gained interest due to their improved properties resulting from the combination of two components in one uniform material.[1] Nanostructured materials have the potential to significantly impact growth in all industries. The dispersion phase of nanocomposites is currently most widely applied as inorganic layered materials.[2–4] The main feature that allows the improved performance is the full dispersion of individual silicate layers with nanoscopic dimensions, known as an exfoliated structure, in a polymer matrix. Layered silicate-based polymer nanocomposites have become attractive organic–inorganic materials owing to their potential as advanced materials. Inorganic layered materials can be categorized as either synthetic materials or natural clays (silicates). Synthetic materials have less impurities, but the price of natural clays is lower and the impurity content can be reduced using appropriate purification processes. Therefore, natural clays composed of multilayered silicates have more potential applications. Among the numerous varieties of natural clay, montmorillonites are widely used in nanofillers, as the electric charge density between the montmorillonite layers is suitable for the use in nanocomposites.[5–7] Due to their high aspect ratio, exchangeable cations between the layers, superior swelling properties, and greater contact area compared with conventional composites, montmorillonites can significantly enhance the heat resistance, and mechanical and gas barrier properties of materials in amounts of approximately 1 to 5 wt%, contributing to their popularity in various industries.[8–10]

Montmorillonite is an inorganic material

composed of hydrophilic silicate layers, but it has low affinity for hydrophobic macromolecules. Consequently, homogeneous mixtures are difficult to achieve when mixing montmorillonites with organic materials. However, in many cases, the silicate layers are not completely dispersed throughout the polymer matrix, and can be better described as intercalated. The formation of nanocomposites has been accomplished by several methods: solution intercalation/exfoliation,[11–14] *in situ* polymerization,[15–23] polymer melt methods,[24–27] etc. Montmorillonites must be modified to obtain homogeneously dispersed materials. Because NH_3^+ is easier to substitute than Na^+, NH_3^+-containing alkylamines can be used to substitute exchangeable Na^+ cations in montmorillonite layers to transform montmorillonites into organoclays. The presence of inorganic cations on the basal planar surfaces of montmorillonite (MMT) layers makes them hydrophilic in nature, and hence renders the clay ineffective for the adsorption of aliphatic and relatively hydrophobic compounds.[28] In addition to hydrophobic effects, organoclays can have expanded spaces between the clay layers and swell to facilitate the diffusion of polymerizing monomers into the galleries of silicate layers during the synthesis process. This method facilitates the stripping of silicate layers, thereby forming delaminated macromolecule/clay nanocomposites. Thus, it is very important to improve the organophilicity for better compatibility with organic polymers. The increased organophilicity of MMT clay results in easy exchange of organic and inorganic cations, thus increasing the distance between the silicate layers.[29]

Boehmite (γ-AlOOH) coating is a thin-layer material that adheres to a parent material to play a special role, and gives anchoring strength to the parent material. It can overcome some defects in the parent material, and improve its surface properties, such as optical characteristics, separation, and filtration properties, erosion and corrosion resistance, wearability and mechanical strength.[30,31] In addition, γ-AlOOH has the advantages of thermal stability, corrosion resistance, high active specific surface area, antioxidation properties, considerable plasticity, and substantial tenacity. In addition to sol–gel approaches, hydrothermal processes belong to a wet-chemical method for preparing boehmite sols.[32] The unique feature of a hydrothermal process is the use of liquid chemical reagents or powder-like samples dissolved in sols as raw materials, instead of conventional powder-like materials. The reactants are homogeneously mixed and reacted in the liquid phase, and the reaction products are stable sols. At present, it is known that γ-AlOOH can induce improved hardness and other properties, and although it has mostly been applied to ceramics as a substrate, recently it has also been applied to other materials.[33–37]

In this report, we describe the preparation and modification of surface-exfoliated montmorillonite and boehmite sol using a hydrothermal method to make boehmite/organomodified MMT (m-MMT) composite materials. Cotton fabric was then coated with these materials, and the weathering, water repellency and conductivity of the processed fabrics were examined to evaluate the effectiveness of boehmite/m-MMT composite materials.

EXPERIMENTAL

Materials

Milled, scoured and bleached plain-weave cotton fabrics [ends (100)*picks (56)/(32^s/1)*(32^s/1)] were kindly provided by the Everest Textile Industry Co., Ltd., Tainan, Taiwan. MMT, cetyltrimethylammonium bromide (CTAB), and aluminum isoproxide (AIP) were purchased from the Acros Co., Ltd., Geel, Belgium. Nitric acid and phosphoric acid were purchased from the Hayashi Pure Chemical Co., Ltd., Osaka, Japan. The scouring agent, laundry detergent (Lipofol TM-1000E), was supplied by the Taiwan Nicca Chemical Industrial Co., Ltd., Taipei, Taiwan.

Preparation and processing

Exfoliation and modification of montmorillonite

In this study, 0.95 g of CTAB was added to 300 mL of deionized water and stirred for 1 h. Phosphoric acid was then added, and the mixture was left to stand for 5 min before adding 10 g of montmorillonite. Next, the mixture was placed in an autoclave and heated under stirring for 24 h to allow ion exchange between the montmorillonite and CTAB for exfoliation. These steps were repeated for the second exfoliation to prepare the final exfoliated and modified montmorillonites. Table 1 summarizes the different reaction temperatures (°C) for exfoliated MMT materials denoted by M_1–M_4.

Preparation of boehmite sol and montmorillonite composites

Exfoliated montmorillonites were weighed and placed in a beaker with boehmite sol. The mixture was stirred by a homogenizer for 10 min to allow homogenous dispersion of exfoliated montmorillonites in the boehmite sol. According to a weight ratio method, 0.02 mol of the boehmite sol was dried, and then 1.8 g of the dried material was combined with 1.8 g (percentage by weight ratio) of exfoliated montmorillonite. Table 2 lists the compositions of hybrid materials M_{11}–M_{15}, M_{21}–M_{25}, M_{31}–M_{35} and M_{41}–M_{45}.

Table 1
Reaction temperatures for exfoliated MMT samples M_1–M_4

MMT	Reaction temperature of exfoliated MMT (°C)			
	30	70	150	200
M_0	M_1	M_2	M_3	M_4

Table 2
Composition of hybrid materials M_{11}–M_{15}, M_{21}–M_{25}, M_{31}–M_{35} and M_{41}–M_{45}

Exfoliated MMT (wt%)	Hybrid of boehmite sol/Exfoliated MMT (M_1-M_4)			
	M_1	M_2	M_3	M_4
5	M_{11}	M_{21}	M_{31}	M_{41}
10	M_{12}	M_{22}	M_{32}	M_{42}
15	M_{13}	M_{23}	M_{33}	M_{43}
20	M_{14}	M_{24}	M_{34}	M_{44}
25	M_{15}	M_{25}	M_{35}	M_{45}

Processing of hybrid materials

Treatment of the cotton fabrics was performed using the "two dips, two nips" padding method, with a pickup of 80%. A padding–drying–curing–finishing procedure was used to disaggregate the agglomerated particles into well-dispersed colloidal particles. Fumed alumina and m-MMT sol-treated fabric samples were padded and nipped to remove the excess liquid and to obtain a wet pickup of 80%, using a padder (Rapid Labortex Co., Ltd., Taoyuan, Taiwan) with a set nipping pressure. The treated fabric was pre-dried in an oven at 80 °C for 3 min. Then, the processed fabrics were cured at 120 °C for 60 s in a preheated curing oven (Chang Yang R3). After curing, the fabrics were placed in 2 g/L scouring agent liquor at 80 °C for 20 min for two washings to thoroughly remove any composite material residue, and dried at 70 °C for 5 min prior to analyses. The processed cotton fabrics, denoted by N_{11}–N_{15}, N_{21}–N_{25}, N_{31}–N_{35} and N_{41}–N_{45}, were gray cotton fabrics coated with composite materials, M_{11}–M_{15}, M_{21}–M_{25}, M_{31}–M_{35} , and M_{41}–M_{45}, respectively.

Methods and characterization

FT-IR spectra were recorded on a Bio-Red Digilab FTS-40 spectrometer (KBr). The ^{29}Si nuclear magnetic resonance (NMR) spectra were collected using a Bruker Avance 400 MHz NMR spectrometer at 78.49 MHz, with a cycle time of 60 s, and 914 scans. The gel films heat treated at various temperatures were analyzed by X-ray diffractometry (XRD), using a Rigaku D/max-RA diffractometer, with CuKα radiation in the range 2θ = 20–90° with 0.02° steps at a scanning speed of 4 scans/min. The surface morphology of the processed cotton fabrics was investigated using field-emission scanning electron microscopy (FE-SEM, Philips XL40). Water contact angle measurements were conducted with a contact angle meter (Sigma CAM100). The weathering properties of the processed textiles were evaluated in accordance with ASTM G154 Cycle 1 testing methods, using a Q-Panel Lab Products QUV-LU-8047 accelerated weathering tester. The surface conductivity of the processed cotton fabrics was analyzed using a high-impedance meter (Mitsubishi, MCP HT450). The operating voltage was 10 V, and the selected probe used URS with a test time of 1 min.

RESULTS AND DISCUSSION

XRD analyses of organomodified montmorillonites

Figure 1 shows the respective XRD patterns of neat MMT and organomodified MMT treated at 30, 70, 150 and 200 °C. When a parallel X-ray beam encounters an orderly arranged interlayered structure, the reflected light may generate constructive interference and increase energy

because of a co-phase (two parallel optical path difference = $n\lambda$), resulting in a relatively strong wave crest in the XRD pattern. For neat MMT (M_o), only a broad scattering pattern at around 2θ = 6.96° was found in the XRD pattern. Figure 1 shows that the wave crest of m-MMT M_4 was shifted to the left after exfoliation at high temperature compared with m-MMT M_1, processed at a lower exfoliating temperature. The interlayer distances d can be calculated according to Bragg's equation; according to calculations, the interlayer distance of montmorillonite M_0 was 1.272 nm (Table 3). The peaks were assigned to the 001 basal reflection. The corresponding basal spacing via the interlayer distance of montmorillonite M_4 increased to 1.805 nm as a result of exfoliation and modification.

Surface morphology of organomodified montmorillonites

Figures 2a–2d show the SEM images of m-MMT at 2000× magnification, which enable the particle sizes and overall distributions in each sample to be compared. Figure 2a illustrates that agglomerates were observed in m-MMT M_1, because the exfoliating temperature was insufficient and the particles could not delaminate, that is, the exfoliation conditions were poor.

Table 3
Interlayer distances of exfoliated MMT materials M_0–M_4

Samples	2θ (degree)	Interlayer distance (nm)
M_0	6.96	1.272
M_1	6.16	1.437
M_2	6.10	1.451
M_3	5.88	1.505
M_4	4.90	1.805

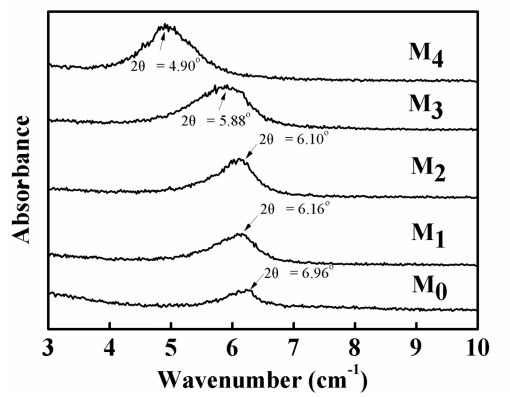

Figure 1: X-ray diffraction patterns of neat and organomodified MMT samples M_0–M_4

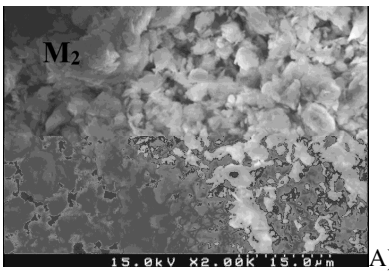

A)

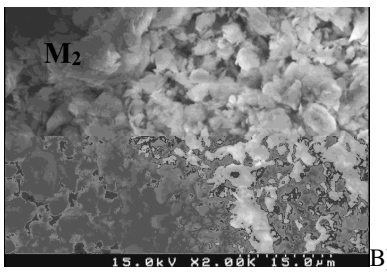

B)

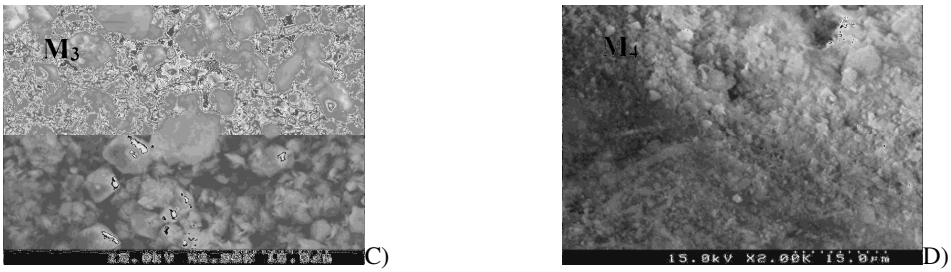

C) D)

Figure 2: SEM images of organomodified MMT samples M_1–M_4; (A) M_1, (B) M_2, (C) M_3, and (D) M_4 (×2000)

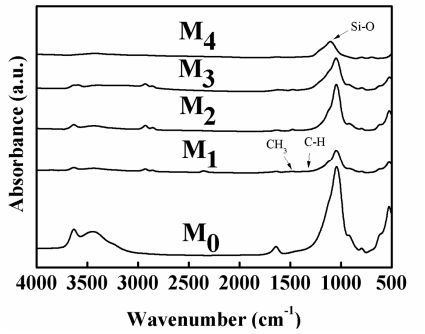

Figure 3: IR spectra of M_0 and organomodified MMT samples M_1–M_4

Table 4
EDS analysis results for materials M_0–M_4

Sample	Elemental composition (%)			
	Al	C	O	Si
M_0	11.49	11.13	32.85	44.53
M_1	8.27	30.26	31.92	29.55
M_2	6.29	35.85	29.79	28.07
M_3	5.99	41.86	28.25	23.90
M_4	4.37	45.68	27.36	22.59

Figure 2c reveals that as the reaction temperatures for m-MMT M_2 (Fig. 2b) and m-MMT M_3 increase, the delamination of particles improves, and the exfoliating angles increase accordingly. As shown in Figure 2d for m-MMT M_4 particles, optimal delamination

Infrared spectra

Figure 3 shows that the neat and organomodified montmorillonites M_0–M_4 have a Si–O absorption peak around 1043 cm^{-1}, a bending vibration of CH_3 groups at 1452 cm^{-1}, and absorption bands at 1381 and 1362 cm^{-1} arising from C–H deformation and asymmetric/symmetric bending, respectively. The Si–O absorption peak was substantially weaker for the exfoliated and modified M_4. When m-MMT M_4 is exfoliated and modified at conditions were achieved when the reaction temperature reached 200 °C. The fine particles allow the adsorption of boehmite sol onto fabrics and a homogeneous coating. This suggests that organomodified montmorillonite was well dispersed within the boehmite sol matrix.

200 °C, hydrolysis and carbonization occur during the preparation process. Exfoliation does not reduce the Si content within the montmorillonite, but the carbon ratio increases substantially under high-temperature exfoliation, resulting in a weaker Si–O absorption peak. When the exfoliation temperature increases, the Si–O absorption peak moves gradually towards longer wavenumbers, proving that the degrees of hydrolysis and carbonization increase as a result of exfoliation.

Elemental analyses

Table 4 lists the elemental analysis results obtained using energy dispersive X-ray spectroscopy (EDS). The data show that the Al, C, and Si contents in montmorillonites exfoliated at different temperatures change with increasing exfoliating temperature. As shown in Table 4, quantitative EDS analysis revealed that the amount of C and O increased due to hydrolysis. Consequently, the fractions of Si and Al decreased because of the gradual increase in the amounts of C and O.

Analysis of ^{29}Si NMR and ^{27}Al NMR spectra

The ^{29}Si NMR spectra of m-MMT in Figure 4 have absorption peaks of Q^2 and Q^4 at δ -96.97 ppm and -109.49 ppm, respectively. The Si–OR signal contains two unreacted Si–OH functional groups out of the four Si bonds in the form of $(H–O)Si(–OSi\equiv)_2$. The four Si bonds in the Q^4 structure of m-MMT reacted completely, and the Si–O functional groups adopted the form $Si(-OSi\equiv)_4$ after the temperature was increased. However, the shapes of the signals at δ -96.40 and -108.96 ppm changed from double to single peaks as the exfoliation temperature increased. From the spectra of m-MMT M_4, the reaction was determined to be almost complete when the exfoliating temperature reached 200 °C. When the number of noise peaks declined and the signals became smoother, the Q^2 peak was transformed almost completely to Q^4, indicating a more complete network structure.

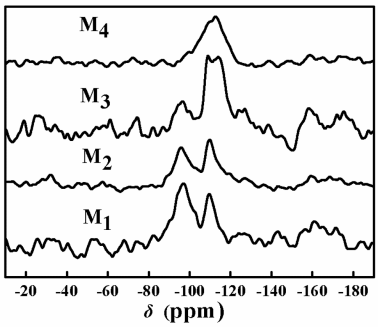

Figure 4: ^{29}Si NMR spectra of organomodified MMT samples M_1–M_4

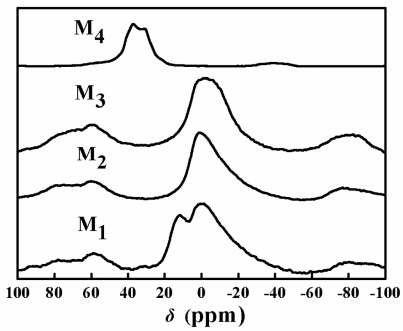

Figure 5: ^{27}Al NMR spectra of organomodified MMT samples M_1–M_4

In the ^{27}Al NMR spectra, the bonds that result from Al hydrolysis are usually six-coordinate bonds at δ -10 to 10 ppm, five-coordinate bonds at 30–50 ppm, and four-coordinate bonds at >50 ppm. As shown in Figure 5, the hybrid materials M_1–M_3 had four-coordinate and six-coordinate bonds at the studied exfoliation temperatures, and six-coordinate bonds gave rise to the main peak at a constant γ-AlOOH ratio at various exfoliation temperatures. It was obvious that the m-MMT M_1–M_3 predominantly contained six-coordinate bonds at low exfoliation temperatures, with a peak at around δ 0.4 ppm. The absorption peak of the four-coordinate bonds was at around δ 58.3 ppm and disappeared gradually with increasing exfoliation temperature. The hybrid material M_4 predominantly contained five-coordinate bonds, which gave rise to an absorption peak at around δ 37.8 ppm at the maximum exfoliation temperature.

Contact angle analysis of processed cotton fabrics

Figures 6–9 present the contact angles of m-MMTs with different amounts of montmorillonite at different exfoliating temperatures and concentrations. The contact angles under different conditions depended on the tested cotton fabrics. Five random sampling points were tested to obtain a mean value. The contact angle of the processed cotton fabrics increased from 133° to 148° when the montmorillonite ratio gradually increased from 5 to 25 wt%. Figure 10 shows a comparison of contact angles at different montmorillonite exfoliation temperatures. With 5 wt% m-MMT, the contact angle of the processed cotton fabric N_{11} was 115° when the exfoliating temperature

was 30 °C, which is the lowest of all the exfoliating temperatures. However, as the exfoliating temperature of montmorillonite increases, the absorption of boehmite sol also increases, and the network structure becomes nearly complete. Therefore, the contact angle of the processed cotton fabric N_{41} increased to 133°, which was the largest value for the m-MMT processed cotton fabrics. We infer that the contact angle increases with increasing montmorillonite exfoliation temperature.

Surface morphologies of processed cotton fabrics

The adhesion of the composite onto the cotton fabric was examined by SEM. Figure 11a shows that the distribution of boehmite sol on the surface of the processed cotton fabric N_{15} was uneven. Consequently, the water repelling efficiency was poor. The amount of boehmite sol coating was greater and the coating was homogeneous for processed cotton fabrics N_{25} (Fig. 11b) and N_{35} (Fig. 11c). For comparison, the montmorillonite particles on the surface of the processed cotton fabric N_{45} are finer and the exfoliation is better because of the higher exfoliation temperature (200 °C), therefore more boehmite sol can be coated on the cotton fabrics (Fig. 11d). In addition, because the montmorillonite particles are finer, their distribution is more homogeneous, which improves the water repellent properties.

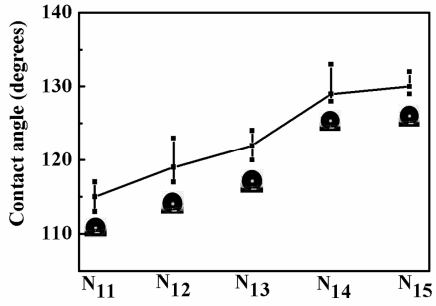

Figure 6: Contact angles of processed cotton fabrics N_{11}–N_{15}

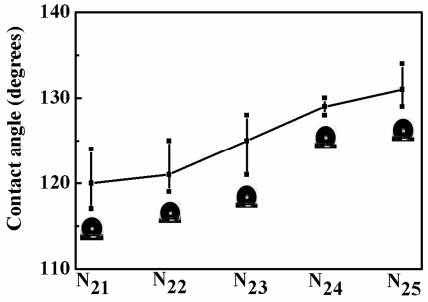

Figure 7: Contact angles of processed cotton fabrics N_{21}–N_{25}

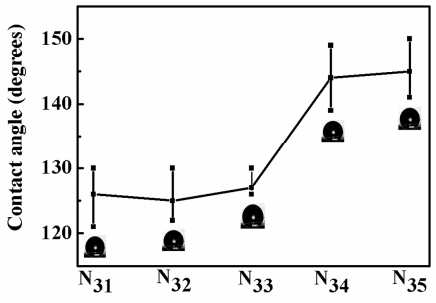

Figure 8: Contact angles of processed cotton fabrics N_{31}–N_{35}

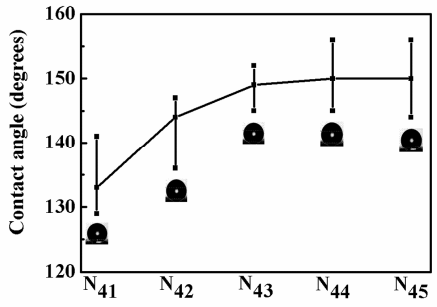

Figure 9: Contact angles of processed cotton fabrics N_{41}–N_{45}

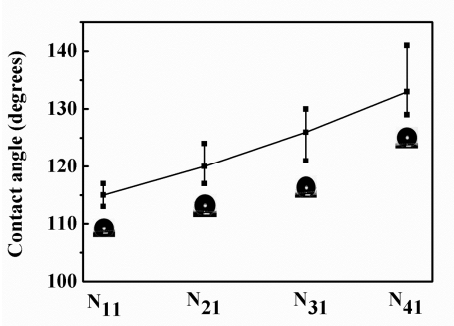

Figure 10: Contact angles of processed cotton fabrics N_{11}–N_{41} at various temperatures

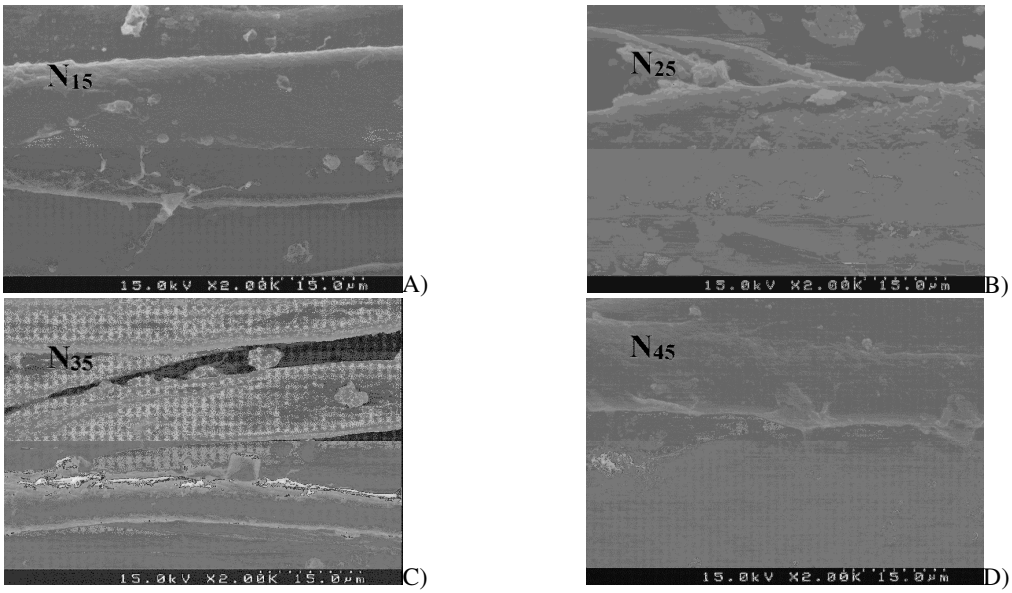

Figure 11: SEM images of processed fabrics N_{15}–N_{45}; (A) N_{15}, (B) N_{25}, (C) N_{35}, and (D) N_{45} at ×2000

Table 5
Conductivities of gray fabrics and hybrid materials processed cotton fabrics N_{11}–N_{15}, N_{21}–N_{25}, N_{31}–N_{35} and N_{41}–N_{45}

Compd.	Conductivity (Ω)	Compd.	Conductivity (Ω)
cotton	1.45×10^{9}	cotton	1.45×10^{9}
N_{11}	4.80×10^{8}	N_{31}	3.14×10^{8}
N_{12}	3.85×10^{8}	N_{32}	2.35×10^{8}
N_{13}	3.45×10^{8}	N_{33}	2.84×10^{8}
N_{14}	3.04×10^{8}	N_{34}	2.89×10^{8}
N_{15}	2.85×10^{8}	N_{35}	1.83×10^{8}
N_{21}	3.68×10^{8}	N_{41}	2.15×10^{8}
N_{22}	3.45×10^{8}	N_{42}	2.94×10^{8}
N_{23}	3.68×10^{8}	N_{43}	2.45×10^{8}
N_{24}	3.26×10^{8}	N_{44}	2.32×10^{8}
N_{25}	2.33×10^{8}	N_{45}	1.54×10^{8}

Table 6
Weathering test results of processed cotton fabrics

Compd.	UV irradiated for 4 h	UV irradiated for 8 h	UV irradiated for 16 h	UV irradiated for 32 h	UV irradiated for 64 h
cotton	4	3-4	3-4	3-4	3-4
N_{11}	4	3-4	3-4	3-4	3-4
N_{15}	4	3-4	3-4	3-4	3-4
N_{21}	4	4	4	4	3-4
N_{25}	4-5	4	4	4	3-4
N_{31}	4-5	4	4	4	4
N_{35}	4-5	4-5	4	4	4
N_{41}	4-5	4-5	4	4	4
N_{45}	4-5	4-5	4	4	4

Conductivity analyses of processed cotton fabrics

To examine the conductivity, composite materials of different ratios were coated on cotton fabrics, and the surface resistance values were measured. A smaller surface resistance value represents better conductivity. The surface resistance of gray cotton fabric was 1.45×10^9 Ω and the conductivity was relatively poor (Table 5). The surface resistance value of the processed cotton fabric N_{11} was 4.80×10^8 Ω, and as the concentration of montmorillonite increased, the amount of adsorbed boehmite sol increased accordingly. The resistance value for the processed cotton fabric N_{15} was 2.85×10^8 Ω. Because boehmite sol contains Al, which can improve conductivity, the conductivity increased moderately. A comparison of the processed cotton fabrics N_{15}, N_{25}, N_{35}, and N_{45} revealed that the resistance values gradually decreased from 4.80×10^8 to 1.54×10^8 Ω. The interlayer spacing expands with higher montmorillonite exfoliating temperatures. Thus, more boehmite sol can be incorporated, improving the conductivity.

Weathering analyses of processed cotton fabrics

Ultraviolet (UV) radiation can be divided into three bands: long-wave UV (also called UVA; 320 or 315–400 nm), medium-wave UV (290–315 or 320 nm), and short-wave UV (100–290 nm). The UV rays that hit the earth have a wavelength of 290–400 nm, because medium-wave UV and short-wave UV are filtered by the ozone layer. They can also cause photofading, photochemical reactions of polymer structures, and polymer degradation.

The weathering tests were conducted for hybrid-material processed cotton fabrics N_{11}–N_{15}, N_{21}–N_{25}, N_{31}–N_{35}, and N_{41}–N_{45}. Based on the ASTM G154 weathering test, the cotton fabric was coated with composite materials at different ratios. The experimental results of the sunlight resistance tests are shown in Table 6. The results for cotton fabric coated with montmorillonite exfoliated at 30 °C and composite N_{11} with 5 wt% boehmite sol indicate that the UV irradiation gray scale for a 64 h test is the same as that of the unmodified cotton fabric. UV resistance did not increase significantly. As the montmorillonite exfoliating temperature for composites increases, the weathering resistance also improves. The optimal UV resistance effect of processed cotton fabrics N_{45}, N_{41}, N_{31}, and N_{35} reached level 4 after 64 h of UV irradiation, because the thin membrane of boehmite sol on the surface of the cotton fabric can prevent UV damage. Therefore, montmorillonite exfoliated at higher temperature can adsorb more boehmite sol, increasing the amount of boehmite sol on processed cotton fabrics. Consequently, the weatherability is greater.

CONCLUSION

In this study, a series of composite materials were prepared, using a hydrothermal method, from boehmite sol and montmorillonite at different concentrations and exfoliating temperatures. Cotton fabrics were coated by the composite materials to investigate the properties of the processed fabrics. XRD revealed that the interlayer distance of montmorillonite increased from 1.272 nm to 1.805 nm by exfoliation and modification with CTAB at 200 °C. NMR and SEM analyses confirmed that higher exfoliating temperatures provided a more complete bonding and network structure. Because boehmite sol can form membranes on the fabric surface and montmorillonite contains Si, the contact angle of the processed cotton fabric was significantly improved. Additionally, the membrane-forming property of boehmite sol also allowed a level 4 weathering effect after 64 h of UV irradiation to be achieved. UV spectra and EDS elemental analysis showed that increasing the exfoliating temperature of montmorillonite causes hydrolysis and carbonization, which increases the C and O contents. Additionally, the conductivity test showed that processed cotton fabrics become more conductive after being coated with composite materials, as the increased alumina content significantly enhanced the electrical conductivity of the processed fabrics, and decreased the resistance tenfold.

ACKNOWLEDGMENTS: The authors would like to thank the National Science Council of the Republic of China, Taiwan, for financially supporting this research under grant NSC 101-2622-E-168-007-CC3.

REFERENCES

[1] C. Sanchez, B. Julian, P. Belleville and M. Popall, *J. Mater. Chem.*, **15**, 3559 (2005).

[2] A. Leszczynska, J. Njuguna, K. Pielichowski and J. R. Banerjee, *Thermochim. Acta*, **454**, 1 (2007).

[3] N. A. Isitman and C. Kaynak, *Polym. Degrad. Stabil.*, **96**, 2284 (2011).

[4] H. Li and D. Y. Gao, *Pigm. Resin Techn.*, **40**, 79 (2011).

[5] L. Solhi, M. Atai, A. Nodehi, M. Imani, A. Ghaemi *et al.*, *Dent. Mater.*, **28**, 369 (2012).

[6] H. M. Chen, J. Chen, L. N. Shao, J. H. Yang, T. Huang *et al.*, *J. Polym. Sci. Pol. Phys.*, **51**, 183 (2013).

[7] D. Manikandan, R. V. Mangalaraja, R. E. Avila, R. Siddheswaran and S. Ananthakumar, *Mater. Sci. Eng. B.*, **177**, 614 (2012).

[8] A. Leszczynska, J. Njuguna, K. Pielichowski and J. R. Banerjee, *Thermochim. Acta*, **454**, 1 (2007).

[9] L. Xie, X. Y. Lv, Z. J. Han, J. H. Ci, C. Q. Fang *et al.*, *Polym. Plast. Technol.*, **51**, 1251 (2012).

[10] B. Jurkowski and Y. A. Olkhov, *Thermochim. Acta*, **414**, 243 (2004).

[11] S. Kim and C. A. Wilkie, *Polym. Adv. Technol.*, **19**, 496 (2008).

[12] H. S. Jeon, J. K. Rameshwaram, G. Kim and D. H. Weinkauf, *Polymer*, **44**, 5749 (2003).

[13] M. Pramanik, S. K. Srivastava, B. K. Samantaray and A. K. Bhowmick, *J. Appl. Polym. Sci.*, **87**, 2216 (2003).

[14] S. Zulfiqar, Z. Ahmad, M. Ishaq and M. I. Sarwar, *Mater. Sci. Eng. A*, **525**, 30 (2009).

[15] Y. Li, B. Zhao, S. Xie and S. Zhang, *Polym. Int.*, **52**, 892 (2003).

[16] M. Huskic and M. Zigon, *Eur. Polym. J.*, **43**, 4891 (2007).

[17] S. Su, D. D. Jiang and C. A. Wilkie, *Polym. Adv. Technol.*, **15**, 225 (2004).

[18] C. Zeng and L. J. Lee, *Macromolecules*, **34**, 4098 (2001).

[19] S. Su and C. A. Wilkie, *J. Polym. Sci. Pol. Chem.*, **412**, 1124 (2003).

[20] S. Ingram, H. Dennis, I. Hunter, J. J. Liggat, C. McAdam *et al.*, *Polym. Int.*, **57**, 1118 (2008).

[21] A. A. Vassiliou, K. Chrissafis and D. N. Bikiaris, *Thermochim. Acta*, **500**, 21 (2010).

[22] A. Rehab and N. Salahuddin, *Mater. Sci. Eng. A*, **399**, 368 (2005).

[23] L. Unnikrishnan, S. Mohanty, S. K. Nayak and A. Ali, *Mater. Sci. Eng. A*, **528**, 3943 (2011).

[24] J. Yu, X. Zeng, S. Wu, L. Wang and G. Liu, *Mater. Sci. Eng. A*, **447**, 233 (2007).

[25] M. Si, M. Goldman, G. Rudomen, M. Gelfer, J. C. Sokolov *et al.*, *Macromol. Mater. Eng.*, **291**, 602 (2006).

[26] J. H. Liaw, T. Y. Hsueh, T. S. Tan, Y. Wang and S. M. Chiao, *Polym. Int.*, **56**, 1045 (2007).

[27] R. R. Tiwari and U. Natarajan, *Polym. Int.*, **57**, 738 (2008).

[28] R. R. Tiwari, K. C. Khilar and U. Natarajan, *Appl. Clay Sci.*, **38**, 203 (2008).

[29] F. Effenberger, M. Schweizer and W. S. Mohamed, *J. Appl. Polym. Sci.*, **112**, 1572 (2009).

[30] A. C. Zaman, C. B. Ustundag and C. Kaya, *J. Eur. Ceram. Soc.*, **30**, 2525 (2010).

[31] S. K. Dhoke, T. J. M. Sinha and A. S. Khanna, *J. Coat. Technol. Res.*, **6**, 353 (2009).

[32] T. Mousavand, S. Ohara, M. Umetsu, J. Zhang, S. Takami, *et al.*, *J. Supercrit. Fluid.*, **40**, 397 (2007).

[33] B. Genoveva and Y. S. Lin, *Micropor. Mesopor. Mat.*, **30**, 359 (1999).

[34] A. Torncrona, J. Brandt, L. Lowendahl and J. E. Otterstedt, *J. Eur. Ceram. Soc.*, **17**, 1459 (1997).

[35] Z. He, J. Mab and G. E. B. Tan, *J. Alloy Compd.*, **486**, 815 (2009).

[36] T. Kiyoharu, K. Noriko and M. Tsutomu, *J. Am. Ceram. Soc.*, **80**, 3213 (1997).

[37] D. Chen and E. H. Jordan, *J. Sol-Gel Sci. Technol.*, **50**, 44 (2009).